Developing an Empirical Relationship to Predict the Strength of Friction Stir Spot Welded Dissimilar Joints of Aluminum Alloy with Carbon Steel

[1]S.Manickam*, [2]C.Rajendran, [3]V.Balasubramanian,

[1]Associate Professor, [2]Project Associate, [3]Professor

Department of Manufacturing Engineering, Annamalai University, Annamalainagar-608002, Tamilnadu, India

*Corresponding Author: Email: sigappimanickam@gmail.com

ABSTRACT

The present investigation aims at developing an empirical relationship to predict the tensile shear strength of friction stir spot welded (FSSW)dissimilar joints of (AA6061 aluminum alloy with carbon steel) incorporating parameters such as tool rotational speed, plunge rate, dwell time and tool diameter ratio. Experiments were conducted according to a four factor, five level central composite rotatable design of experiments concept. Strength of the joint was evaluated by a single lap shear test. Analysis of variance (ANOVA) technique was used to check the adequacy of the developed relationship. The developed empirical relationship can be effectively used to predict tensile shear strength of the joints at 95% confidence level.

Keywords : Friction stir spot welding; Response surface methodology; Aluminum alloy; Mild steel; Tensile shear fracture load.

1.0   INTRODUCTION

The joining of dissimilar materials like aluminum and steel is becoming an important research topic in automotive industries because of the need for high strength to weight ratio, corrosion resistance and crash resistance. However, the welding of these two dissimilar materials is very difficult due to variation in physical and chemical properties, and, especially, the different melting temperatures. Adhesive bonding is used to join these combinations of materials in automobile industry to avoid the formation of brittle intermetallics (Fe_nAl_m) [1]. This problem can be overcome by friction stir spot welding (FSSW) process, a variant of friction stir welding (FSW) process, patented by The Welding Institute (TWI), U.K [2]. In FSSW, the temperature needed to join aluminum with carbon steel lies below the solidus line of aluminum alloy (AA6061), and, so, FSSW provides many advantages over the conventional fusion welding processes [3-5].

The principle of FSSW process is illustrated in **Fig. 1**. A non-consumable rotating tool, with a probe pin, plunges into the upper sheet first and then in to the lower sheet (**Fig. 1a**). The tool rotational speed and axial force are maintained for a short duration (dwell time) to generate frictional heat between the tool shoulder and work piece (**Fig. 1b**). Due to the frictional heat, the softened material, adjacent to the tool, deforms plastically, and a solid state bond is produced between the upper and lower sheets. Finally, the tool is withdrawn from the joint (**Fig. 1c**) [6].
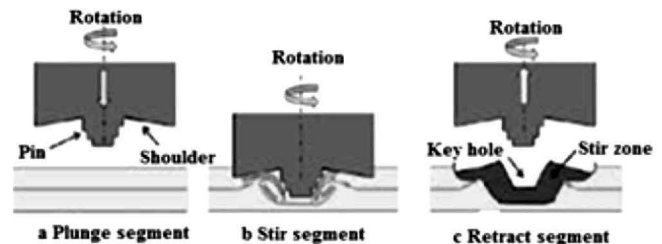

Fig.1 : Schematic diagram of FSSW process

Bozzi et al. [7] investigated the effect of intermetallic compound (IMC) layer in Al 6016/IF steel friction stir spot welding (FSSW). They identified different types of IMC at the interface such as $FeAl_3$, Fe_2Al_5 and $FeAl_2$. This IMC improves the mechanical properties, but a thick IMC layer initiated crack propagation at the interface. Choi et al. [8] analyzed the formation of IMC in Al and Mg alloy interface, and reported that the formation of IMC at the interface between Al/Mg had significant effect by the FSSW parameters. It was found that a thick IMC layer (Al_3Mg_2, $Al_{12}Mg_{17}$) seriously reduces the joint strength. Sun et al. [9], who obtained the microstructure and mechanical properties of dissimilar Al Alloy/Steel joints performed by the flat spot FSW, reported the absence of IMC in the nugget region, but the presence of areas with amorphous atomic configuration along the Al/Fe joint interface due to low heat input. It was observed that the failure occurred through nugget pullout, at a maximum tensile shear fracture load (TSFL) of 3.6 kN.

Babu et al. [10] investigated the effect of tempered conditions of base material (AA2014) on the joint strength and the optimized FSSW process. Karthikeyan et al [11] optimized FSSW process parameters such as tool rotational speed, plunge rate, plunge depth and dwell time on AA2024 aluminum alloy using response surface methodology (RSM), and attained the maximum tensile shear fracture load (TSFL) of 9.39 kN. Ramanjaneyulu et al. [12] optimized the yield strength, tensile strength and ductility of friction stir welded AA2014-T6 aluminum alloy using RSM, and also found that AA2014-T6 aluminum alloy welded with hexagonal tool pin profile showed the highest tensile strength and elongation compared to the conical, triangle, square, and pentagon pin profiles. Plaine et al [13] reported the effect of process parameters on the strength of Al/Ti joints using full factor factorial design of experiments and ANOVA, and found that the tool rotational speed was the parameter with the greatest influence on the joint strength, followed by the dwell time. The effect of tool rotational speed and dwell time on the joint interface microstructure and tensile shear strength of friction stir spot welded Al-5083 aluminum/ St-12 steel alloy sheets was investigated by Fereidui et al. [14].

Many researchers worldwide have already applied RSM to optimize friction stir welding process parameters in similar and dissimilar alloys [7-14]. However, the information available in open literature on FSSW of dissimilar joints (especially aluminum alloys and carbon steel)are very sparse. Keeping this in mind, the present investigation was carried out to join AA6061 aluminum alloy with carbon steel by FSSW process and an attempt was also made to develop an empirical relationship to predict strength (tensile shear fracture load) of the welded joints incorporating FSSW parameters by Response Surface Methodology (RSM).

2.0 EXPERIMENTAL PROCEDURE

The base materials used in this investigation were the rolled sheets of 2.45 mm thick AA6061 aluminum alloy (in T6 condition) and 3 mm thick carbon steel. The chemical composition of the base materials are presented in **Table 1.** The mechanical properties of the base materials are presented in **Table 2**, based on preliminary work and from the literature [11-14].

Table 1 : Chemical composition (wt. %) of base materials

Alloy	C	S	P	Zn	Ti	Fe	Cu	Al	Mn	Si	Mg
Carbon steel	0.09	0.02	0.01	-	-	Bal.	-	-	0.22	-	-
Aluminum alloy	--	--	--	0.25	0.15	0.7	0.25	95.8	0.33	0..66	1.10

Table 2 : Mechanical properties of base materials

Alloy	0.2% Yield strength (MPa)	Ultimate Tensile strength (MPa)	Elongation in 50 mm gauge length (%)	Hardness @ 0.05 kg @ 0.05 kg load (HV)
Carbon steel	379	483	18	185
Aluminum alloy	276	310	12	107

The independent process parameters affecting the strength of FSSW joints were identified. They are tool rotational speed (N), plunge rate (R), dwell time (T) and tool diameter ratio (D). The tool diameter ratio is the ratio between shoulder diameter to pin diameter. Shoulder is the primary heat generating source due to larger contact area with the abutting surfaces. Pin is the secondary heat generating source due to the vertical flow of the stirred material and plasticization of the material around the pin. Hence, the tool diameter ratio (shoulder and pin) play a vital role in controlling the frictional heat generation and, subsequently, on the resultant microstructure and mechanical properties. The feasible limit of each process parameter was determined in such a way that the joint should be free from visible defects. The upper limit of the each process parameter was coded as +2 and lower limit as -2. The intermediate coded values can be calculated using the following relationship,

$$X_i = 2 [2X - (X_{max} + X_{min})] / (X_{max} - X_{min}) \qquad (1)$$

where X_i is the required coded value of a variable X; X is any value of the variable from X_{min} to X_{max}; X_{min} is the lower limit of the variable and X_{max} is the upper limit of the variable. The selected process parameters with limits are presented in **Table 3**.

Table 3 Important FSSW parameters and their levels

Sl. No	Factor	Unit	Notation	Levels				
				-2	–1	0	+1	+2
1	Tool Rotational speed	rpm	N	800	900	1000	1100	1200
2	Plunge Rate	mm/min	R	2	3	4	5	6
3.	Dwell Time	sec	T	3	4	5	6	7
4	Tool diameter ratio	--	D	2.0	2.5	3.0	3.5	4.0

The selected design matrix is shown in **Table 4**. It is a four-factor, five-level central composite rotatable design matrix (CCD) consisting of 30 sets of coded conditions and composed of 16 factorial points, 8 star points and 6 center points. The 30 experimental runs allowed the estimation of the linear, quadratic and two way interactive effects of the process parameters on tensile shear fracture load (TSFL). During trial experiments, Al sheet was kept as the top sheet, but resulted in distortion and insufficient bonding between Al and steel. Moreover, the aluminum sheet easily attained plastic state before the steel sheet attains plastic state due to low heat input supplied to bottom sheet. Due to the direct contact between the tool shoulder and top surface of the steel sheet, the high heat input was supplied to plasticize the steel sheet and less heat input to the Al sheet. This resulted in proper stirring between the steel and Al sheet. Hence, the steel sheet was kept as the top sheet and Al sheet was kept as the bottom sheet in this investigation. Tool wear was not observed in this investigation. This may be due to two reasons. They are: (i) the tool material used was high speed steel (SHSS), which is harder than mild steel sheet, and (ii) the FSSW is an intermittent process and not a continuous welding process like FSW.

Tools with five different shoulder diameters (**Fig.2**) were fabricated using super high speed steel (SHSS). In each experimental condition, three Al/Steel dissimilar joints were fabricated and they are tested. The average of three results is presented in **Table 4**.


Fig.2 : Fabricated FSSW tools with various shoulder diameter

Table 4 Design matrix and Experimental Results

Exp. No.	Coded value					Original Value			TSFL (kN)
	N	R	T	D	N	R	T	D	
1	-1	-1	-1	-1	900	3	4	2.5	6.33
2	+1	-1	-1	-1	1100	3	4	2.5	6.75
3	-1	+1	-1	-1	900	5	4	2.5	6.90
4	+1	+1	-1	-1	1100	5	4	2.5	7.73
5	-1	-1	+1	-1	900	3	6	2.5	7.29
6	+1	-1	+1	-1	1100	3	6	2.5	7.41
7	-1	+1	+1	-1	900	5	6	2.5	7.65
8	+1	+1	+1	-1	1100	5	6	2.5	8.21
9	-1	-1	-1	+1	900	3	4	3.5	6.95
10	+1	-1	-1	+1	1100	3	4	3.5	7.45
11	-1	+1	-1	+1	900	5	4	3.5	7.48
12	+1	+1	-1	+1	1100	5	4	3.5	8.26
13	-1	-1	+1	+1	900	3	6	3.5	7.82
14	+1	-1	+1	+1	1100	3	6	3.5	8.41
15	-1	+1	+1	+1	900	5	6	3.5	8.31
16	+1	+1	+1	+1	1100	5	6	3.5	8.40
17	-2	0	0	0	800	4	5	3	6.12
18	+2	0	0	0	1200	4	5	3	7.21
19	0	-2	0	0	1000	2	5	3	7.06
20	0	+2	0	0	1000	6	5	3	8.44
21	0	0	-2	0	1000	4	3	3	8.39
22	0	0	+2	0	1000	4	7	3	9.76
23	0	0	0	-2	1000	4	5	2	5.87
24	0	0	0	+2	1000	4	5	4	6.85
25	0	0	0	0	1000	4	5	3	9.46
26	0	0	0	0	1000	4	5	3	9.13
27	0	0	0	0	1000	4	5	3	9.18
28	0	0	0	0	1000	4	5	3	9.07
29	0	0	0	0	1000	4	5	3	9.28
30	0	0	0	0	1000	4	5	3	9.37

The pin diameter and pin length were maintained at 5 mm. The profile on the pin was tapered threaded (left hand). All the specimen were welded, as per the conditions dictated by the design matrix,on an indigenously designed and developed computer numerical controlled friction stir welding machine (6 Ton capacity). The aluminum sheet was used as bottom sheet and mild steel sheet was used as top sheet in lap joint configuration (**Fig. 3**). The fabricated FSW welded joints are shown in **Fig. 4**.
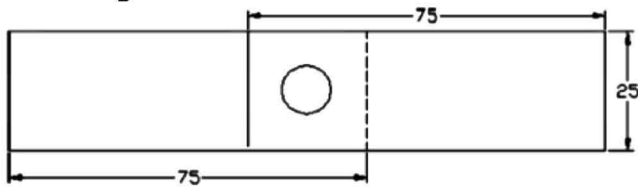
(All dimensions are in mm)
Fig. 3 : FSSW joint configuration

Fig.4 : Fabricated FSSW joints

3.0 DEVELOPMENT OF EMPIRICAL RELATIONSHIP

The response (Y), the tensile shear fracture load (TSFL) of FSSW joints is, a function of tool rotational speed (N), plunge rate (R), dwell time (T) and tool diameter ratio (D) and, hence, can be expressed as

$$Y=f(N, R, T, D) \qquad (2)$$

For the selected four factors and the interaction factors, the selected polynomial can be expressed as

$$Y=b_0+b_1N+b_2R+b_3T+b_4D+b_{11}N^2+b_{22}R^2+ \\ b_{33}T^2+b_{44}D^2+b_{12}NR+b_{13}NT+b_{14}ND+b_{23}RT+ \\ b_{24}RD+b_{34}TD \qquad (3)$$

Where b_0 is the average of responses and b_1, b_2... b_4, b_{11}, b_{13}... b_{44} are the regression coefficients that depend on the main and interaction effects of parameters. DESIGN EXPERT 9.1

software was used to calculate the values of these coefficients, presented in **Table 5**.

Table 5 Co-efficients and its estimated factors

Coefficient	Factor Estimate
Intercept	9.25
N-Tool rotational speed	0.25
R- Plunge rate	0.30
T- Dwell time	0.35
D-Tool diameter ratio	0.28
NR	0.039
NT	-0.073
ND	-1.8
RT	-0.078
RD	-0.056
TD	-3.1
N^2	-0.63
R^2	-0.35
T^2	-0.023
D^2	-0.70

After determining the coefficients, the empirical relationship to predict TSFL was developed. The developed empirical relationship in the coded form indicating all the coefficients, is given below :

$$TSFL = \{9.25+0.25N+0.30R+0.35T+0.28D+0.039NR \\ -0.073NT -1.8ND -0.078RT-0.056RD -3.1TD -0.63N^2 \\ -0.35R^2-0.023T^2-0.70D^2\}kN \qquad (4)$$

The adequacy of the developed empirical relationship was tested using the analysis of variance (ANOVA) technique with the help of DESIGN EXPERT 9.1 software. The ANOVA test results are presented in **Table 6**. The F-value of the developed model is 168.65 implies the model is significant. There is only a 0.01% chance that the F-value of a model this large could occur due to noise. Values of "Prob> F" less than 0.05 indicate that the model terms are significant. In this case, N, R, T, D, NT, RT, RD, N^2, R^2, T^2 and D^2 are significant model terms. The lack of fit F-value of 1.27 implies that the lack of fit is not significant relative to the pure error. Non-significant lack of fit is good. The co-efficient of determination R^2 values gives the goodness of

fitness of the model. For a good model, R^2 value should be close to 1. In this model the calculated R^2 value is 0.98. This implies that 98% of the experimental data confirms with the data predicted by the developed model. The value of the adjusted R^2 of 0.97 is also high, which indicates a high significance of the model. The predicted R^2 value is 0.94, which shows reasonable agreement with the adjusted R^2 value of 0.97. Adequate precision measures the signal to noise ratio, and a ratio greater than 4 is desirable. The value of 34.714 in this case indicates that this model can be used to navigate the design space. **Fig. 5** shows the cross sections of FSSW joints at the lower, medium and higher TSFL values. The experimental TSFL values and corresponding predicted TSFL values of the responses are close to each other as presented in the correlation graph in **Fig. 6**, which indicates the prediction capabilities of the developed empirical relationship.
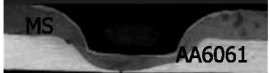
Joint No.	Micrograog	TSFL (kN)
23	MS AA6061	5.87
13	MS AA6061	7.82
25	MS AA6061	9.46

Fig.5 : Cross-sectional macrograph of the FSSW joints

Table 6 : ANOVA test results

Source	Squares	df	Square	F-Value	Prob> F	
Model	31.87	14	2.28	186.65	<0.0001	significant
N	1.54	1	1.54	58.45	<0.0001	
R	2.21	1	2.21	84.30	<0.0001	
T	2.93	1	2.93	111.66	<0.0001	
D	1.91	1	1.91	72.70	<0.0001	
NR	0.025	1	0.025	0.94	0.3466	
NT	0.086	1	0.086	3.26	0.0912	
ND	5.6E-05	1	5.6E-5	2.1E-3	0.9637	
RT	0.098	1	0.098	3.72	0.0730	
RD	0.050	1	0.050	1.88	0.1900	
TD	1.5E-04	1	1.5E-04	5.9E-03	0.9395	
N^2	10.73	1	10.73	408.58	<0.0001	
R^2	3.44	1	3.44	131.06	<0.0001	
T^2	0.015	1	0.015	0.55	0.4684	
D^2	13.51	1	13.51	514.26	<0.0001	
Residual	0.39	15	0.026			
Lack of Fit	0.28	10	0.028	1.27	0.4170	not significant
Pure Error	0.11	5	0.022			
Cor. Total	32.26	29				
Std. Dev.	0.16	R-Squared		0.9878		
Mean	7.88	Adj. R-Squared		0.9764		
C.V. %	2.06	Pred. R-Squared		0.9445		
PRESS	1.79	Adeq. Precision		34.714		

Table 7 : Validation test results

Expt. No.	Tool rotational speed(N) in rpm	Plunge rate (R)in mm/min	Dwell time (T) in sec	Tool Diameter ratio (D)	TSFL (kN)		Error (%)
					Actual	Predicted	
1	1015	4.3	6	3	9.45	9.51	-0.63
2	1020	4.2	6	3	9.64	9.68	-0.41
3	1030	4.5	6	3	9.62	9.48	1.45
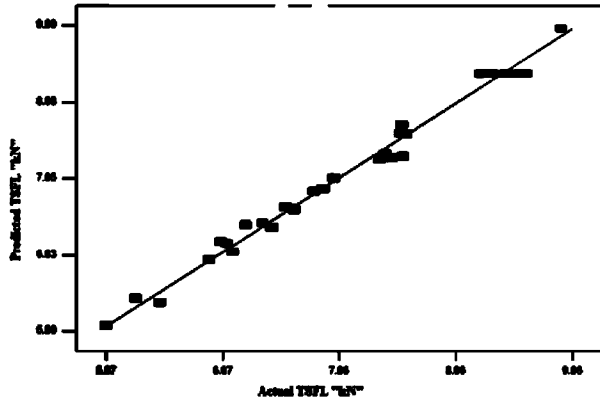
Fig.6 : Correlation graph

The lower tool rotational speed, high tool plunge rate, low dwell time and low tool diameter ratio (lower heat input condition) produce inadequate heat due to lower friction between the tool shoulder and weld line, which results in poor plastic flow of material in nugget and formation of defect in the nugget zone. Moreover, two different types of fracture modes were observed under lap shear loading: nugget de-bonding and nugget pull-out. The nugget de-bonding occurred in joints with a low heat input, whereas nugget pullout was observed in other conditions. It can be observed that the increase of hook width increases the tensile shear fracture load, whereas the increase of hook height decreases the tensile shear fracture load, irrespective of process condition. The hook initiation distance from the tool interface of the joints is generally found to increase with the increase of tensile shear fracture load. The peak temperature variation due to the changes in process parameters affected stir zone width along the interface in the weld region in addition to stir zone volume. Consequently, the hook width and the effective top sheet thickness were changed according to the process parameters and the variations in geometrical features determine the modes of failure, and resulted in corresponding fracture values [15].

The long hook width and deep effective top sheet thickness

yielded high fracture load whereas short hook width and shallow effective top sheet thickness yielded low fracture load. As the stir zone width is high it offers more resistance to fracture along the interface through bonding region, while the crack propagation depends on the hook orientation and final fracture is completed through the shortest distance of either the effective top sheet thickness or bonded region in lap shear tensile loading [16]. It is observed that the actual resisting area formed at the faying surfaces depends on the heat input, the forging force and the duration of the weld cycle. These lead to different modes of failure and finally influence the fracture values. On loading, crack propagation is initiated from the boundary between the upper and lower sheets, progresses along the region of mechanical bonding, grows through the metallurgical bond and finally reaches the SZ, where failure occurs. This defect acts as the crack initiation location during shear test, and so, the TSFL is lower. The higher tool rotational speed, high dwell time, and high tool diameter ratio (higher heat condition) produce excess heat that causes for metallurgical changes such as grain coarsening [17] re-dissolution and coarsening of strengthening precipitates at the nugget [18] and lower dislocation density [19-22] that decrease the TSFL value. **Table 7** presents the actual and predicted values of TSFL. **Fig. 7** illustrates the perturbation plot for the response TSFL of FSSW joints.
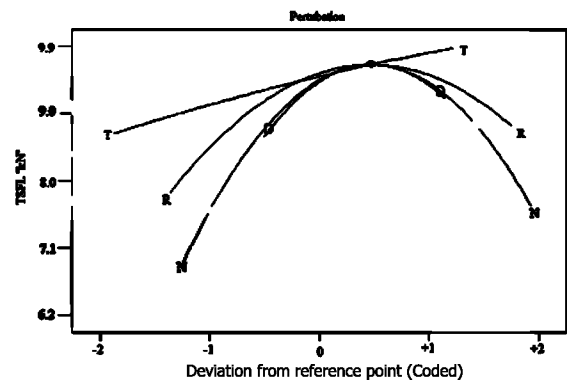

Deviation from reference point (Coded)

Fig.7 : Perturbation plot showing the effect of parameters on the TSFL

This plot provides silhouette view of the response surface and shows the change of TSFL while parameter moves from the reference point, with all other parameters held constant at the reference value.

Fig. 8(a) show the IMC layer of the FSSW of Al/Fe joint fabricated at the tool rotational speed of 1000 rpm, plunge rate of 4 mm/min, dwell time 5 sec and diameter ratio of 3, and thickness of IMC layer is 4µm. **Fig.8 (a)** revealed that the hardness measurement across the IMC layer and presented different hardness (188 Hv), this brittle IMC layer may be act as the crack initiation point during tensile testing. Hence, the fracture mode is nugget plug-out. **Fig. 8 (b)** shows the SEM fractograph of fractured surface, it revealed that large no of cleavage, which suggests that the fracture mode is brittle.
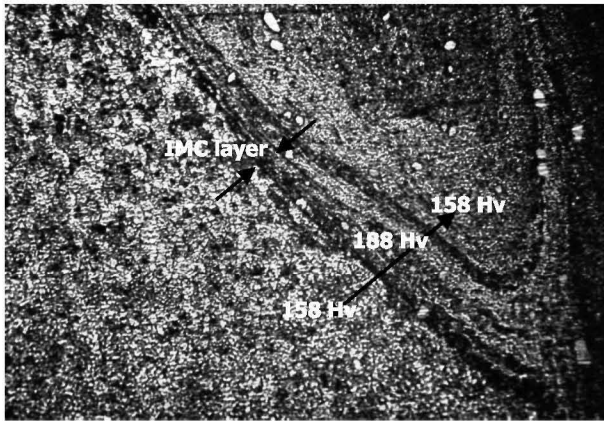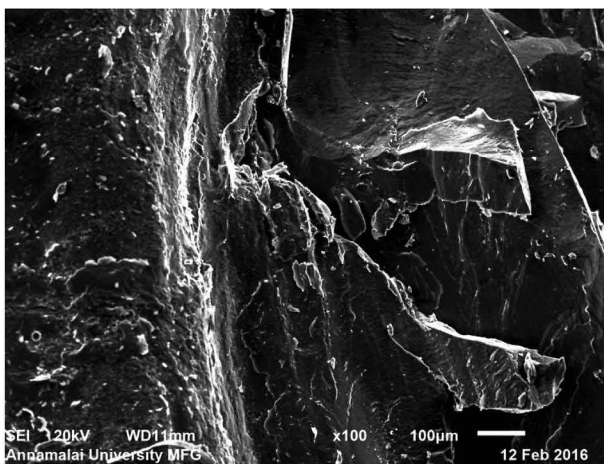

Fig.8 (a) : Microstructure of Stir Zone

Fig.8 (b) : SEM fractograph

4.0 CONCLUSIONS

1. An empirical relationship was developed to estimate the tensile shear fracture load (strength) of friction stir spot welded dissimilar joints of AA6061 aluminum alloy and carbon steels incorporating important process parameters. This relationship can be effectively used to determine the TSFL at 95% confidence level.

2. The maximum TSFL value of 9.46kN was exhibited by the joint fabricated using, tool rotational speed of 1000 rpm, plunge rate 4 mm/min, dwell time of 5 sec and tool diameter ratio of 3.

3. Of the four process parameters investigated, the dwell time was found to have the greatest influence on tensile shear fracture load, followed by plunge rate, tool diameter ratio and tool rotational speed (as per the F ratio).

REFERENCES

[1] Gunter F., Vallant R., Weinberger T., Enzinger N., Schröttner H. and Paśič H. (2009): Friction Stir Spot Welds between Aluminium and Steel Automotive Sheets: Influence of Welding Parameters on Mechanical Properties and Microstructure, Welding in the World, Vol. 53, pp R13-R23

[2] Thomas W. M. and Nicholas E. D. (1997): Friction stir welding for the transportation industries. Material Design, Vol. 18, pp. 269-73.

[3] Dupont J. N., Banovic S. W. and Marder A. R. (2003): Microstructural Evolution and Weldability of Dissimilar Weld between a Super Austenitic Stainless Steel and Nickel-Based Alloys, Welding Research, pp. 125-135.

[4] Sato Y. S., Nelson T. W., Sterling C. J., Steel R. J. and Pattersson C.-O. (2005): Microstructure and mechanical properties of friction stir welded SAF 2507 super duplex stainless steel, Material Science Engineering A, Vol. A397, pp.376-384.

[5] Uzun H., Dalle Donne C., Argagnotto A., Ghidini T. and Gambaro C. (2005): Friction stir welding of dissimilar Al 6013-T4 to X5CrNi18-10 stainless steel, Materials Design, Vol. 26, pp.41-46.

[6] Wang D.A. and Lee S.C. (2007): Microstructures and failure mechanisms of friction stir spot welds of

aluminum 6061-T6 sheets, J. of Material Processing Technology, Vol. 186, pp.291-297.

[7] Bozzi A, Helbert-Ettera, A.L., T. Baudinb, B. Criquic, J.G. Kerbiguetc, (2010): Intermetallic compounds in Al 6016 /IF-steel friction stir spot welds, Materials Science and Engineering A, Vol. 527, pp.4505-4509

[8] Don-Hyun Choi, Byung-WookAhn, Chang-Yong Lee, Yun-Mo Yeon, Keun Song, Seung-Boo Jung (2011): Formation of intermetallic compounds in Al and Mg alloy interface during friction stir spot welding, Intermetallic, Vol. 19, pp.125-130.

[9] Y.F. Sun, H. Fujii, N. Takaki, Y. Okitsu (2013): Microstructure and mechanical properties of dissimilar Al alloy/steel joints prepared by a flat spot friction stir welding technique Materials & Design, Vol. 47, pp.350-357.

[10] Babu S., Sankar V. S., Janaki Ram G. D., Venkitakrishnan P.V., Madhusudhan Reddy G. and Prasad Rao K. (2013): Microstructures and Mechanical Properties of Friction Stir Spot Welded Aluminum Alloy AA2014, J. of Materials Engineering Performance, Vol. 22(1), pp. 71-84.

[11] Karthikeyan R. and Balasubramanian V. (2010): Predictions of the optimized friction stir spot welding process parameters for joining AA2024 aluminum alloy using RSM, Int. J. of Advanced Manufacturing Technology, Vol. 51, pp.173-183.

[12] Ramanjaneyulu K., Madhusudhan Reddy G. and Gokhale H. (2015): Optimization of process parameters of aluminum alloy AA 2014-T6 friction stir welds by response surface methodology, Defence Technology, Vol. 11, pp. 209-219.

[13] Planine A.H., Gonzalez A.R., Suhuddin U.F.H., Dos Santos J.F. and Alcantara N.G. (2015): The optimization of friction spot welding process parameters in AA6181-T4 and Ti6Al4V dissimilar joints, Materials & Design, Vol. 83, pp.36-41.

[14] Fereiduni E., Movahedi M. and Kokabi A.H. (2015): Aluminum/steel joints made by an alternative friction stir spot welding process, J. of Materials Processing Technology, Vol. 224, pp.1-10.

[15] Badarinarayan H, Yang Q and Zhu S (2009): Effect of tool geometry on static strength of friction stir spot-welded aluminum alloy, International Journal of Machine Tools and Manufacture, Vol. 49(2), pp.142-148.

[16] Tozaki Y, Umematsu Y and Tokaji K, (2007): Effect of processing parameters on static strength of dissimilar friction stir spot-welds between different aluminum alloys. Fatigue and Fracture of Engineering Materials and structures, Vol. 30, pp.143-148.

[17] Bozukurt Y., Salman S. and Cam G. (2012): Investigation of friction stir spot weld of AA2024 and AA5754 Al alloy sheets, Science and Technology of Welding and Joining, Vol. 18, pp.337-345.

[18] Khuri A.I. and Cornell J. A. (1987): Response Surfaces, Dekker, New York.

[19] Raj Kumar S., Muralidharan C. and Balasubramanian V. (2010): Establishing empirical relationship to predict grain size and tensile strength of friction stir welded AA6061-T6 aluminum alloy joints, Transaction of Non-ferrous Materials Society of China, Vol. 20, pp.1863-1872.

[20] Lomolino S., Tovo R. and Dos Santos J. (2005): On the fatigue behaviour and design curves of friction stir butt welded Al alloys, Int. J. of Fatigue, Vol. 27, pp. 305-316.

[21] Benavides S., LI Y., Murr L.E., Brown D. and McClure J.C. (1998); Low temperature friction stir welding of 2024 Aluminum, Scripta Materialia, Vol. 41, pp. 809-815.

[22] Threadgill P.L. (1997) : Friction stir welds in aluminum alloys - preliminary microstructural assessment, TWI Bulletin, TWI, Abington, Cambridge, UK, Industrial Report No.: 513/2/97.